HiSST: 3rd International Conference on
High-Speed Vehicle Science Technology
14 -19 April 2024, Busan, Korea

# Interaction of Mainstream Injection with Boundary Layer Combustion for Hydrogen Fuel

*J. Sandral[1], T. Vanyai[2], A. Veeraragavan[3], V. Wheatley[4]*

## Abstract

Boundary layer combustion in scramjet flow paths is often disrupted from strong flow features such as a mainstream injector. Experiments were conducted, investigating the effect a mainstream injector has on boundary layer combustion initiated by a porous plate and multi-porthole injector array. Hydrogen was injected at representative flow rates in a 2D ducted flow path to allow for visualization of the flow. High speed schlieren imaging, chemiluminescence and planar laser induced fluorescence characterized the flow structure, while thin film heat transfer gauges and pressure gauges measured the level of combustion. Both the MPIA and porous plate were disrupted along the centerline behind the mainstream injector but were unaffected off the centerline axis. The porous plate was able to achieve earlier combustion and produced a more uniform layer of burning fuel in comparison to the MPIA.

**Keywords**: *Hypersonic, Hydrogen, Boundary Layer, Combustion, Porous*

## Nomenclature

Latin
I – Impulse
St – Stanton number
M – Mach number
P – Pressure
U – Velocity
T- Temperature
x – Streamwise direction
y – Spanwise direction
z – Vertical direction

Greek
Ø – Diameter
Superscripts
H – A superscript
Subscripts
sp – Specific

## 1. Introduction

Film injection of fuel and subsequent boundary layer combustion (BLC) is a proposed solution to mitigate the high skin friction drag, and heat loads, generated inside a scramjet flow path. An analytical solution first published by Stalker in 2005 [1] and expanded by Barth et al. [2] predicted skin friction reductions greater than 50% for hydrogen. Combustion within the boundary layer adds heat locally, reducing the local density. This reduction both expands the boundary layer and alters the turbulent transport closer to the wall, both phenomena providing a barrier to momentum transport between the wall and high-speed flow above. Successfully realizing this effect in scramjets would provide a significant boost to net $I_{sp}$, with minimal alteration to vehicle design. Numerical studies ranging in complexity from Large Eddy Simulations (LES) to Reynolds Averaged Navier Stokes (RANS) simulations have also verified these reductions, investigating the alteration of turbulent transport [3] and relative heat addition in the boundary layer compared to the mainstream flow [4]. Experimental investigations directly or indirectly measured the skin friction drag on representative flow paths [2-6], also validated the potential for large

[1] *Centre for Hypersonics, University of Queensland, St. Lucia, QLD, Australia, uqjsandr@uq.edu.au*
[2] *Centre for Hypersonics, University of Queensland, St. Lucia, QLD, Australia*
[3] *Centre for Hypersonics, University of Queensland, St. Lucia, QLD, Australia*
[4] *Centre for Hypersonics, University of Queensland, St. Lucia, QLD, Australia*

reductions of drag. However, a study attempting to implement BLC into a prototype accelerating engine flow path did not measure the expected reduced skin friction [10]. The layer of fuel injected into the boundary layer was disrupted by a turn in the engine flow path. Mainstream injection may also act as a strong flow disrupter to BLC due to the strong vortices generated behind the point of injection as seen in Fig. 1. These strong vortices can alter the layer of fuel injected into the boundary layer, removing the fuel from proximity to the wall, reducing the overall effectiveness of BLC. Slot injection has been the injector of choice for previous BLC experiments, due to the ease of implementation within a given flow path [7-11]. However, alternative injectors such as a porous plate provide an additional benefit of replenishing fuel within the boundary layer as it is disrupted from the vortices of the mainstream injectors. This interaction is illustrated in Fig. 1, where the vortices from the mainstream injector weaken further downstream and porous plate continues to inject fuel into the boundary layer.

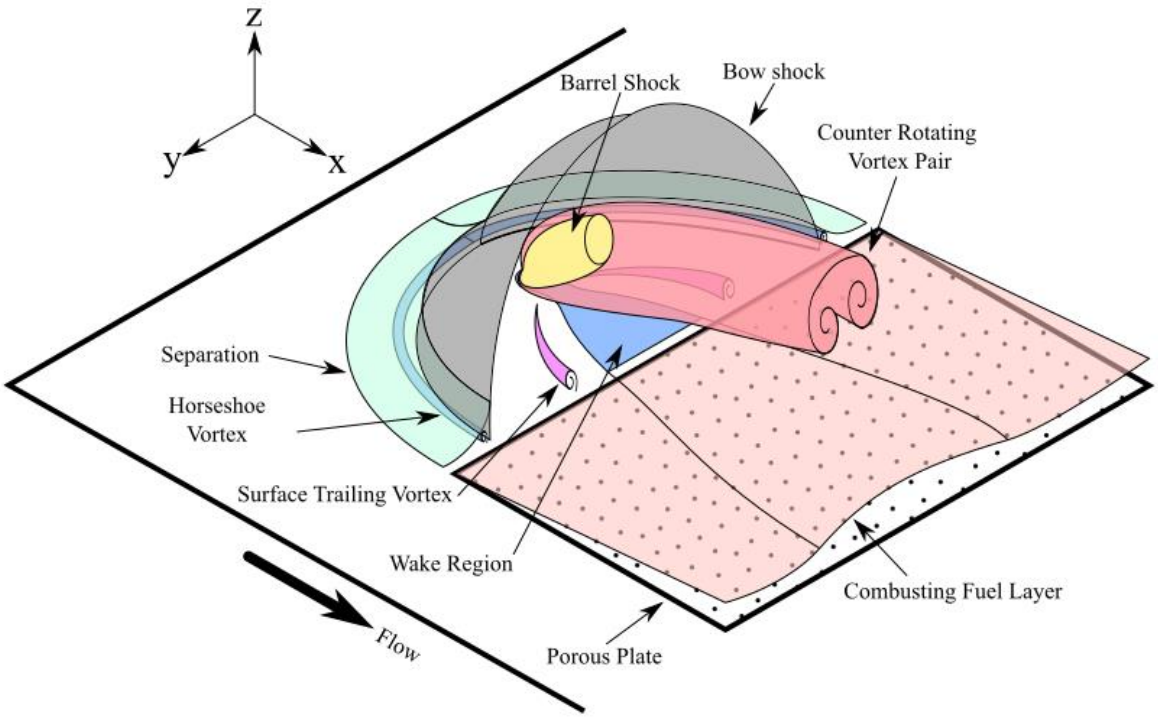


**Figure 1.** *Mainstream injector interaction with a porous plate adapted from [12] and updated from [13].*

Experiments were conducted with a porous plate and in conjunction with a mainstream injector with optical measurements taken to quantify the state of the flow and understand how BLC develops in the presence of a mainstream injector. To provide comparison, a Multi-Porthole Injector Array (MPIA) is also tested. MPIAs have been proposed as an alternative instigator of BLC [11]. The additional vortices and complex flow structure generated by the array will provide better near field mixing of the fuel, while the low equivalence ratios will ensure it remains within the boundary layer.

## 2. Methodology

### 2.1. Facility and Model

Experiments were conducted in the T4 Stalker Tube, or T4, at the University of Queensland. T4 is a reflected shock tunnel capable of producing flight stagnation enthalpy matched hypersonic flow conditions, for approximately 2 – 4 ms. Measurements taken during an experimental run, or shot, are passed through a facility calculator to account for changes in flow properties due to the high pressures and temperatures generated. These properties are listed in Table 1 as nozzle exit conditions for the facility nozzle that produces a nominally Mach 4 test flow. The outflow of the facility was compressed via a symmetric pair of 6.5° ramps to ensure sufficient combustion occurs within the field of view of the optical measurements. Pressure measurements taken at the throat of the experimental model are then used to calculate the compressed flow conditions via the oblique shock equations using the nozzle exit

conditions. These are listed in Table 1 as model throat conditions. To support optical access a rectangular duct of constant area was necessary to provide flat mounting surfaces for windows. The mainstream injector was placed upstream of an insert that could accommodate a porous plate or MPIA injector. Behind the injectors, a sensor plate is mounted housing thin film heat transfer gauges, Kulite pressure gauges and skin friction gauges. Heat transfer is presented as a Stanton number (St) based upon the mainstream flow properties passing over the gauges through the model. The pressure values are measured as an absolute pressure. The skin friction results are presented as normalized values between different fueling conditions. Fig. 2 depicts the model labeled with key features. Note the top diagram is oriented differently to the bottom two diagrams with unfueled schlieren field of view included.

**Table 1.** Flow conditions of facility and experimental model.

| Test Gas | M (-) | P (kPa) | U (m/s) | T (K) |
|---|---|---|---|---|
| Nozzle Exit | 3.91 | 38.0 | 2347.0 | 930.5 |
| Model Throat | 3.07 | 120.1 | 2227.4 | 1306.6 |

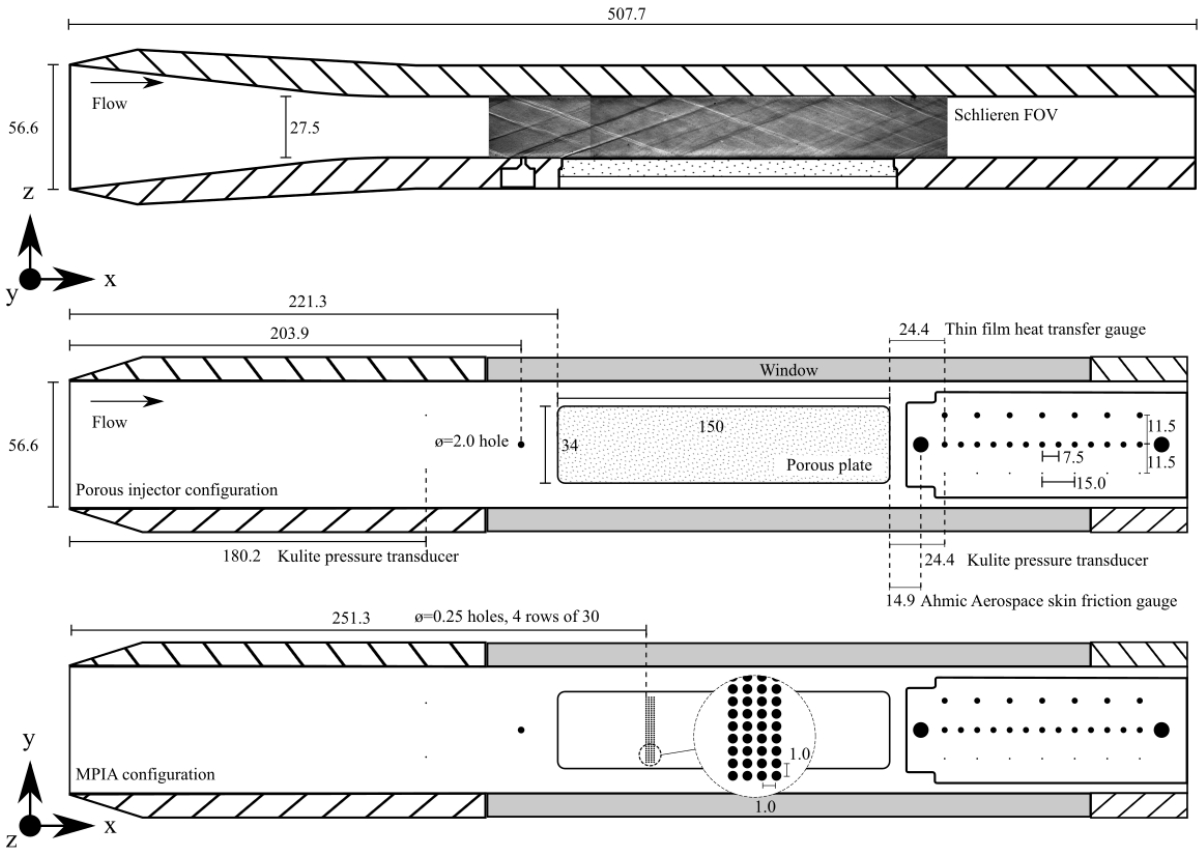


**Figure 2.** *Experimental model schematic.*

Three separate visualization techniques were utilized throughout the experiments to produce a complete picture of the flow during each experiment and the field of views for each optical technique is shown in Fig. 3. High speed schlieren imaging shows how the flow evolved over the test and validated the test had a steady mean flow. The frame rate of the camera was approximately ~80kHz and the light source was a high-powered laser that illuminated the flow for 10ns for each frame captured. The Planar Laser Induced Fluorescence (PLIF) system utilized an Nd:YAG laser to pump a dye laser tuned to a wavelength of 283.92nm. This wavelength targets the OH radical that will be produced from combustion in the flow. The laser sheet was aligned to the centre of the flow path to capture information of the combusting fuel being disturbed from the vortices behind the mainstream injector. Additionally, the gaussian of the PLIF sheet was recorded on a separate dye cell during the experiments and used to correct the captured image such that the intensity is normalized for the varying laser sheet power.

After this correction, the edges of the laser sheet did not have enough signal and were clipped further. The physical edges of the laser sheet are noted in all PLIF images as magenta lines for clarity. Details of this optical system is covered in [14]. Chemiluminescence was captured on the same camera as the PLIF signal with a long exposure without the presence of the laser sheet. This will describe broad regions of where combustion is occurring during the test, integrating across the span of the model and in time. The laser power and camera settings were kept consistent for all tests, including both PLIF and chemiluminescence imaging. Therefore, changes in signal intensity are associated to changes in radicals and combustion intensity.

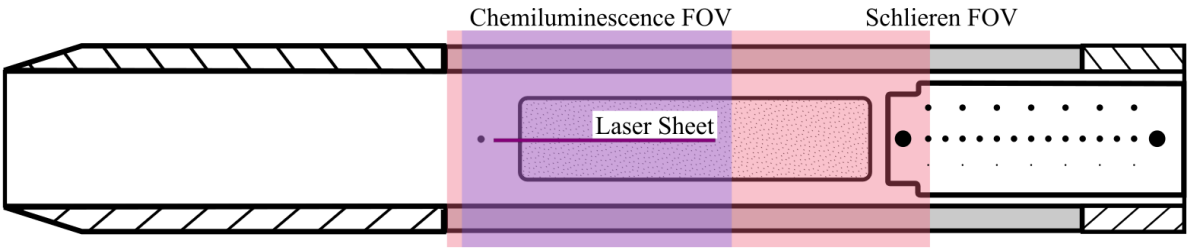


**Figure 3.** *Field of view of optical techniques (Red = Schlieren FOV, Blue = Chemiluminescence, Purple = PLIF laser sheet).*

The mainstream injector and porous plate or MPIA were supplied from two different fuel supplies, therefore the fueling rates could decoupled. For these experiments the mainstream injector flow rate was held constant at an equivalence ratio of 0.18. The porous plate and MPIA were held constant at an equivalence ratio of 0.05 global equivalence ratio. Based on an estimation of the boundary layer thickness, this corresponds to a boundary layer localized equivalence ratio of 0.8.

## 3. Results

The results presented as images were acquired across different experimental runs in T4, with the fueling configurations and conditions held constant for repeatability. The PLIF and chemiluminescence images are overlayed on top of a schlieren image taken during the test time. The sensor data presented are averages acquired over multiple runs.

The base case for the PLIF measurements was the mainstream injector in isolation. As seen in Fig. 4, two regions of turbulence are seen located at the edge of the fuel plume and adjacent to the wall. These regions agree well with the turbulence seen in the schlieren images and where the boundary of the fuel plume is. The turbulent region close to the wall also corroborates the turbulent structures that would disrupt a layer of fuel in the boundary layer. The next image in Fig. 3, shows porous injection in isolation. The structure of the combustion radicals is a diffuse layer close to the wall, with minimal disruption from the main flow. The combustion appears to be uniform and even through the boundary layer and lines up with the bright region that is seen in the schlieren that was attributed to combustion. The lack of turbulent structures in the porous injected layer of fuel is unique and when compared to the mainstream injector indicates relatively small mixing with the mainstream air. This validates that porous injection can promote BLC with minimal disruptions to the mainstream flow. The final image in Fig. 4 shows the combination of mainstream and porous injection. The resultant flow field of combustion products appears to be additive in nature, with the features of both combining. Turbulent features on the edge of the fuel plume were still visible and did not appear altered. Close to the wall, there appears to be a mixture of the two injectors with a more uniform layer of fuel from the porous injection at x = 275mm, however the upper boundary of this diffuse layer has some turbulence that appears to be breaking the layer of fuel up. Further evidence of the BLC being disturbed by the mainstream injector is provided from the lack of bright region in the boundary layer. Therefore, the porous plate is able to resist some of the disruptive effects of the mainstream injector.

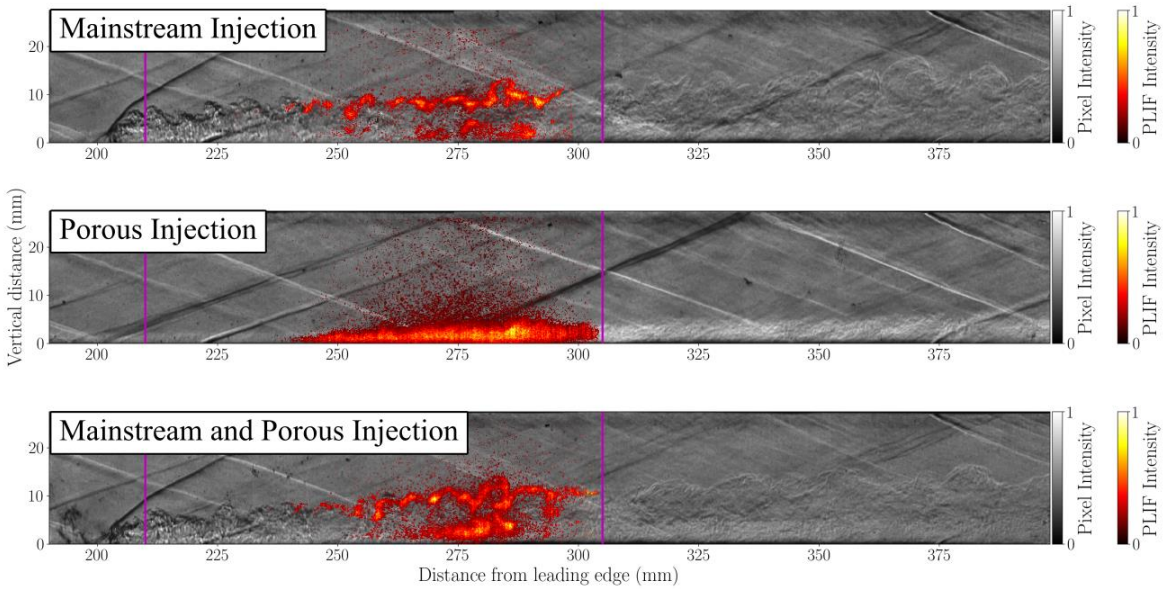


**Figure 4.** *PLIF of porous plate injection configurations.*

Fig. 5 shows the results of the chemiluminescence images. The signals measured in these images are integrated across the span of the experimental model and over 0.2ms of flow time. Therefore, no turbulent structures are expected to be visible and instead the images provide insight into where combustion is occurring. The location of combustion in the flow agrees with the PLIF measurements, with extra information on how combustion begins at the mainstream injector. For the porous injection case the same diffuse layer of combusting fuel was seen within the boundary layer. However, based on the pixel intensity, the combustion is more robust at x = 270mm where the shock reflects. This may be attributed to the unignited fuel that was injected further upstream being consumed. The combustion then equalizes to the level of combustion seen at x = 300mm as fuel is consumed and replenished by the porous plate. These measurements also validated the additive nature of the two injectors when used together. The mainstream injector in isolation had an even region of combustion that filled half of the experimental duct. However, the addition of the porous plate injection increased the brightness of the flow adjacent to the wall indicating additional combustion was occurring within the boundary layer.

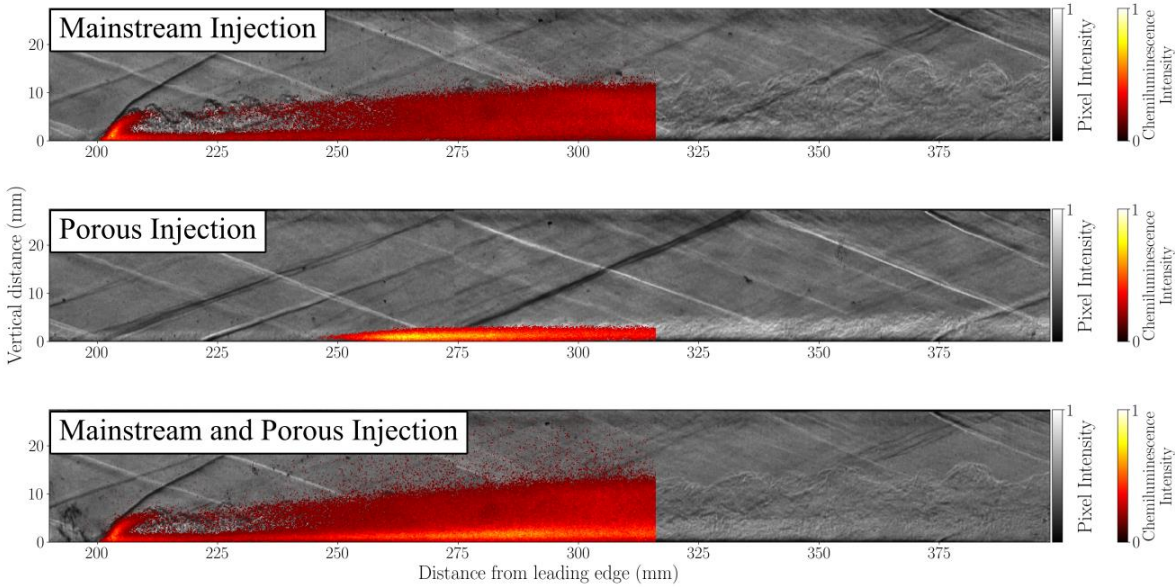


**Figure 5.** *Chemiluminescence of the porous injection schemes.*

Contrasting the effectiveness of the porous plate to produce BLC, the same tests were conducted with an MPIA placed instead. This MPIA was replicated from a previous design that had been shown to promote reliable BLC within a short flow path [15]. Fig. 6 shows the compilation of PLIF images that were acquired with this experimental configuration. The first notable change from the porous was the lack of combustion from the MPIA when it was being used in isolation. From the Schlieren images combustion began just after the laser sheet, with small amounts of signal being measured from the PLIF at x = 300mm. Once the MPIA ignited, the combustion was more robust in comparison to the porous plate with a weak visible shock being generated at x = 310mm. Another contrast to the porous plate configuration, was the change in combustion that MPIA experienced when used in conjunction with the mainstream injector. The mainstream injector behaved as pilot for the MPIA and provided a shield for the MPIA from the core flow. The MPIA then produced combustion deeper within the core flow, with a clear barrier between the wall and the region of combustion. This may diminish the effectiveness of the BLC to reduce shear stress within the boundary layer. The mainstream injector was also disrupted by the MPIA, with fuel plume being displaced by the MPIA and turbulent structures altered.

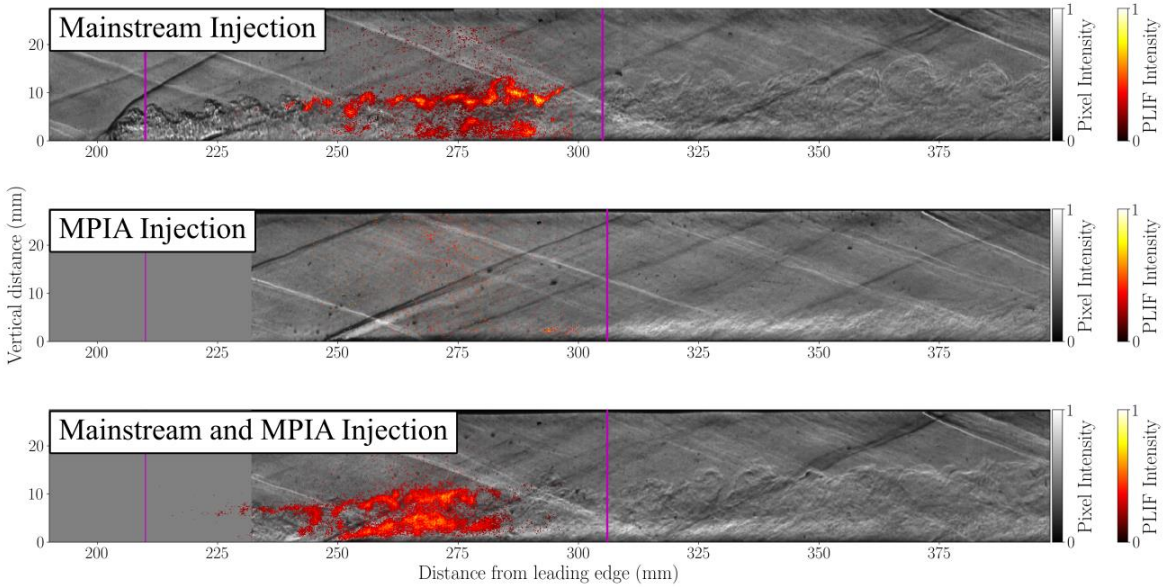


**Figure 6.** *MPIA injection compilation.*

One of the potential benefits to BLC is the reduction of heat transfer to the wall of the flow path from the hypersonic flow. This is achieved by the reduction of shear stress reducing the heat transfer and outweighing and added heat transfer from proximity to combustion. However, this is only applicable to high enthalpy flows, where the heat transfer from skin friction is comparatively large [1]. For these experiments, reduction in heat transfer is not expected and instead increases of heat transfer are attributed to combustion occurring within proximity to the wall from BLC. Fig. 7 shows the average heat transfer measurements downstream of the porous plate or MPIA for each fueling configuration as a Stanton number. Measurements were limited to the centerline gauges and display how changing fueling configuration changes the measured heat transfer. Unfortunately, due to the harsh nature of the flow, many of the heat transfer gauges were damaged during the experimental campaign. These are omitted from the following plot. To confirm the measurements are due to proximity of combustion to the heat transfer gauges and not due to bulk flow heating from combustion, heat transfer gauges were placed on the opposite side of the experimental model where no combustion or fuel is likely to penetrate. Comparisons between fueling configurations did not indicate any larger increases in heat transfer on the unfueled wall, with marginal increases being measured in cases where mainstream injection was used.

From experimental runs where the MPIA and porous plate were in isolation, there is a clear increase in heat transfer when compared to the unfueled case. This indicates the fuel is still in close proximity to the wall and persists after the point of injection and FOV of the optical techniques. The mainstream injector in isolation does increase combustion adjacent to the wall, however not to the extent the porous plate or MPIA does despite more fuel being injected. This effect is also seen any time the mainstream injector was used with the porous plate or MPIA, indicating the mainstream injector is very disruptive

and dominates the heat transfer affects far downstream. Therefore, despite the porous plate appearing to resist some of the mainstream injector effects and replenishing fuel within the boundary layer, once the fuel stops being injected the mainstream injector continues to remove the fuel layer.

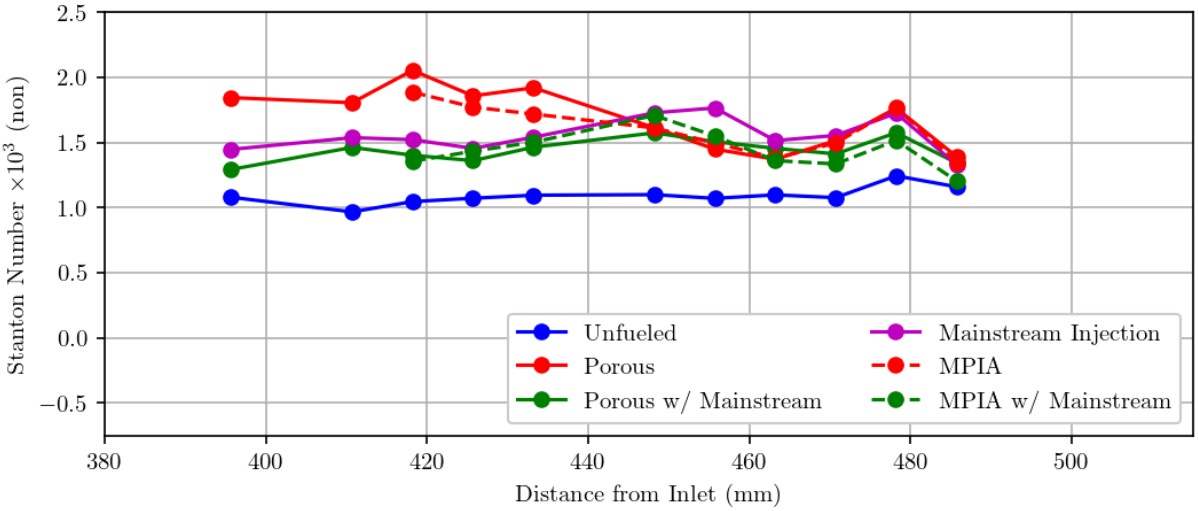


**Figure 7.** *Centerline heat transfer results for all fueling configurations.*

To better understand how mainstream injector affects BLC over the span of the flow path, additional sensors were placed towards the edge of the porous plate insert. The width of the mainstream injectors region of influence was visually confirmed during the experiments from deposition of soot that lined up with the horseshoe vortex generated at the bow shock. This was shown to fill the full width of the porous plate insert, thereby exerting its influence over all the injected fuel from the porous plate or MPIA. Fig. 8 shows all the heat transfer measurements acquired off the centerline of the model. The porous plate and MPIA in isolation both produced higher heat transfer measurements in comparison to the unfueled configuration. Therefore, both injectors produced a uniform layer of fuel across the span of the experimental model. The mainstream injector in isolation also marginally increased the heat transfer over the unfueled case as seen along the centerline measurements. The main difference to the centerline measurements are the fueling cases where the mainstream injector is used with the porous plate and MPIA. Along this section of the flow path, the MPIA and porous plate injected fuel is unaffected by the presence of the mainstream injector. The heat transfer measurements are the same or marginally higher than these injectors in isolation. This indicates the trailing vortices generated by the mainstream injector are disruptive directly behind the point of injection but do not expand beyond 11.5mm to disturb the flow.

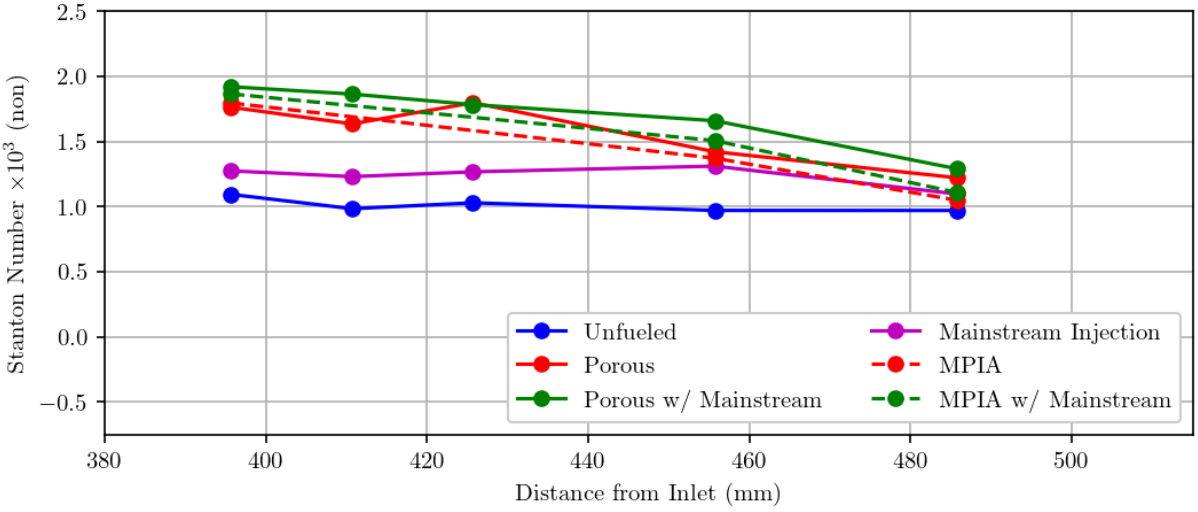


**Figure 8.** *Off Centerline heat transfer results for all fueling configurations.*

Two skin friction gauges, directly behind the porous insert and prior to the exit of the model, were installed to confirm reductions in shear stress were being generated. Unfortunately, due to the short

test time of the facility, the gauges were not able to reach stable measurements within the experimental test time. Due to this, we could not measure precise data. Despite this, the response from the gauges were repeatable and sensitive to changes in fueling configurations. Comparisons between fueling configurations were then conducted by normalizing the average measured signal over the facility test time against an upper bound and lower bound encountered across fueling configurations. In all measurements, the unfueled case was assumed to be the largest skin friction value and so assigned a value of 1. For the porous injection case in isolation, the resultant trace was lower than the combustion suppressed case and so assigned a value of 0. The measurement acquired for combustion suppressed case then fell between the unfueled and combustion on case. From Table 2, this was closer to the unfueled with a value of approximately 0.8 over both skin friction gauges. This indicates the layer of fuel injected by the porous plate was uniform and persisted over the entire flow path until the exit of the model. In contrast, the MPIA injection case had a comparable reduction of shear stress at SF1, however by the time it had reached SF2 the fuel had likely been either consumed or transported away from the wall and approached the unfueled case without the help of combustion to keep the shear stress low. This indicates the MPIA may be more suitable for targeted reductions of shear stress but less suitable for global reductions. The column on the right shows the effect the mainstream injector had on these measurements. Porous plate seemed least disturbed by the presence of the injector, with the measured shear stress at SF1 being increased slightly relative to porous injection only. However, this then decreases further downstream until prior to the exit of the model the shear stress had approached a similar value that had been measured when the porous injection was being done in isolation. The MPIA exhibited a similar behavior however was less effective at resisting the disturbances generated by the mainstream injector.

**Table 2.** Skin friction results, unfueled was taken to be a value of 1.

| **Injection Scheme** | **Combustion Suppressed** | | **Mainstream Injection Included** | |
|---|---|---|---|---|
| | SF1 | SF2 | SF1 | SF2 |
| Porous Injection = 0 | 0.77 | 0.79 | 0.37 | 0.07 |
| MPIA Injection = 0 | 0.68 | 0.96 | 0.65 | 0.34 |

The pressure measurements validated the experimental model had minimal angle of attack and yaw relative to the outflow of the facility nozzle. Additionally, for the porous and MPIA injection case there was minimal combustion induced pressure rise due to the low fueling rates. Combustion was confirmed via optical techniques instead.

## 4. Conclusions

In conclusion, the porous plate and MPIA behaved similarly downstream once all the fuel had been injected and combustion had begun. From the optical techniques utilized both produce robust combustion within the boundary layer, however with different use cases in mind. The porous plate is likely more desirable for global reductions of shear stress due to the diffuse and even layer of combustion being promoted. In contrast the MPIA will be more useful to target regions of high shear stress along a flow path. Achieving this by producing robust combustion and in turn reductions of shear stress at specific locations, however quickly diminishing as all the fuel is consumed and is unable to be replenished. The mainstream injector was an effective disrupter to the layer of fuel being injected, with the heat transfer measurements being dominated by the effects the mainstream injector had on the flow. However as seen by the off-axis heat transfer measurements this was likely limited to immediately behind the point of injection and both the MPIA and porous plate were able to effectively fuel boundary layer combustion elsewhere despite the presence of the mainstream injector. From optical measurements, the porous plate was more resistant to these disturbances with increased regions of combustion close to the wall remaining over the porous plate and sensor measurements indicate combustion persists beyond the length of the porous plate.

**Acknowledgements**

This research was a collaboration between the Commonwealth of Australia (represented by the Defence Science and Technology Group) and the University of Queensland, funded through a Defence Science Partnerships agreement. The authors also acknowledge the T4 technician Keith Hitchcock for his support setting up experiments. Acknowledgment is given to the T4 tunnel operators: Hugh Russell and Matt Trudgian. Acknowledgment is also given to Oliver Street for support during optical setup.

## References

1. Stalker, R.: Control of Hypersonic Turbulent Skin Friction by Boundary- Layer Combustion of Hydrogen. Journal of Spacecraft and Rockets (2005). https://doi.org/10.2514/1.8699
2. Barth, J. E., Wheatley, V., and Smart, M. K.: Hypersonic Turbulent Boundary-Layer Fuel Injection and Combustion: Skin-Friction Reduction Mechanisms. AIAA Journal (2013) https://doi.org/10.2514/1.j052041
3. Denman, A.: Large-Eddy Simulation of Compressible Turbulent Boundary Layers with Heat Addition". Ph.D. thesis, University of Queensland, 2007.
4. Chan, W. Y. K., "Effects of flow non-uniformities on the drag reduction by boundary layer combustion," Ph.D. thesis, University of Queensland, 2012.
5. Goyne, C. P., Stalker, R., Paull, A., and Brescianini, C. P.: Hypervelocity Skin-Friction Reduction by Boundary-Layer Combustion of Hydrogen. Journal of Spacecraft and Rockets (2000). https://doi.org/10.2514/2.3645
6. Rowan, S. A.: Viscous Drag Reduction in a Scramjet Combustor. Ph.D. thesis, The University of Queensland, 2003.
7. Suraweera, M. V., Mee, D., and Stalker, R.: Skin Friction Reduction in Hypersonic Turbulent Flow by Boundary Layer Combustion. 43rd AIAA Aerospace Sciences Meeting and Exhibit (2005). https://doi.org/doi:10.2514/6.2005-613
8. Kirchhartz, R. M., "UpstreamWall Layer Effects on Drag Reduction with Boundary Layer Combustion," Ph.D. thesis, University of Queensland, 2009.
9. Chan,W.Y. K., Mee, D., Smart, M. K., and Turner, J. C.: Effects of flowdisturbances from cross-stream fuel injection on the drag reduction by boundary layer combustion. AIAA Journal (2012). https://doi.org/10.2514/6.2012-5889
10. Barth, J. E., Wise, D. J., Wheatley, V., and Smart, M. K.: Tailored Fuel Injection for Performance Enhancement in a Mach 12 Scramjet Engine. Journal of Propulsion and Power (2018). https://doi.org/10.2514/1.b36794
11. Pudsey, A. S., Boyce, R. R., and Wheatley, V.: Hypersonic Viscous Drag Reduction via Multiporthole Injector Arrays. Journal of Propulsion and Power (2013). https://doi.org/10.2514/1.b34782.
12. Gruber, M. R., Nejad, A. S., Chen, T. H., and Dutton, J. C., "Mixing and Penetration Studies of Sonic Jets in a Mach 2
13. Viti, V., Neel, R., and Schetz, J. A., "Detailed flow physics of the supersonic jet interaction flow field," Physics of fluids (1994),Vol. 21, No. 4, 2009, pp. 46101–46116.
14. Vanyai, T., Brieschenk, S., Bricalli, M., Sopek, T., and McIntyre, T. J., "Thermal compression effects within a fundamental, hydrogen-fuelled scramjet," Aerospace science and technology, Vol. 110, 2021, p. 106499. https://doi.org/10.1016/j.ast.2021.106499. Freestream," Journal of propulsion and power, Vol. 11, No. 2, 1995, pp. 315–323.
15. Pudsey, A. S., Wheatley, V., and Boyce, R. R., "Supersonic Boundary-Layer Combustion via Multiporthole Injector Arrays," AIAA Journal, Vol. 53, No. 10, 2015, pp. 2890–2906. https://doi.org/10.2514/1.j053817.